INTERNATIONAL JOURNAL OF COMMUNICATION SYSTEMS
Int. J. Commun. Syst. 2016; **29**:1305–1322
Published online 18 December 2015 in Wiley Online Library (wileyonlinelibrary.com). DOI: 10.1002/dac.3100

Throughput maximization in electromagnetic energy harvesting cognitive radio sensor networks

Ozgur Ergul[1,*,†], Fatih Alagoz[2] and Ozgur B. Akan[1]

[1]*Next-generation and Wireless Communications Laboratory, Department of Electrical and Electronics Engineering Koc University, Istanbul, 34450 Turkey*
[2]*Department of Computer Engineering Bogazici University, Istanbul, 34342 Turkey*

SUMMARY

In the near future, billions of wireless devices are expected to be operational. To enable the required machine to machine communications, two major problems must be addressed. How to obtain the required spectrum efficiency, and how to deliver the required power to these devices. The most promising answers to these questions are cognitive radio and energy harvesting, respectively. Energy harvesting enables deployment of sensors and devices without having to worry about their battery lifetime. Cognitive radio increases the utilization of spectrum by accessing unused spectrum dynamically. Energy harvesting from electromagnetic waves is suitable for these low power, low cost devices used in machine to machine communications because only minimal additional hardware is required for such energy harvesting. With this idea as the starting point, we first present an analysis on how much throughput can be obtained from a cognitive, electromagnetic energy harvesting wireless network. Then, we show when and how cooperation among network nodes may increase performance. We believe that our results will provide insight for the development of future cooperative cognitive energy harvesting networks. Copyright © 2015 John Wiley & Sons, Ltd.

Received 13 May 2015; Revised 5 September 2015; Accepted 10 November 2015

KEY WORDS: energy harvesting; cognitive radio; machine to machine communications; stochastic network geometry

1. INTRODUCTION

Energy harvesting (EH) techniques considerably increase the lifetime of wireless devices. Theoretically, EH enables infinite energy gain. However, because this gain is obtained at a limited rate, that is, harvesting power, energy efficiency is still one of the major concerns for EH devices. Even though there is an extensive amount of work in the literature on energy efficient communication schemes, they generally address conventional battery operated devices. There is a key difference between them and EH devices. While the former is restricted by energy inside the battery, the latter has infinite energy but is restricted by harvesting power. Because their restrictions and abilities differ from conventional battery operated wireless devices, EH devices need solutions tailored specifically for them.

Energy harvesting in wireless communications has, in fact, been a hot topic in the recent years. Related research is mostly focused on finding optimal methods under certain assumptions on network conditions. Some of these works assume perfect knowledge of EH profile at the transmitter and present optimal resource allocation methods for various objective functions [1–3]. Others assume statistical knowledge of the EH profile and try to optimize with regard to stability regions, in which, both data and energy queues are kept bounded so that the system can keep on operating [4, 5].

*Correspondence to: Ozgur Ergul, Next-generation and Wireless Communications Laboratory, Department of Electrical and Electronics Engineering, Koc University, Istanbul, 34450 Turkey.
†E-mail: ozergul@ku.edu.tr

Natural sources such as sun, wind underwater currents, and acoustic waves are considered for EH in these works. With their infinite energy, natural sources are good targets for EH. However, EH from these sources require additional equipment to be placed on the nodes. Moreover, these sources are not consistent on the amount of energy they provide due to day–night cycles, seasonal changes and overall dependency on environmental conditions.

More recently, EH from electromagnetic (EM) waves has been considered as an alternative to these natural sources. Because harvesting can be performed via the existing antenna of the node, this method offers a significant advantage in terms of cost, size, weight, and ease of implementability. However, because the amount of energy harvested from EM waves is lower than the energy that can be harvested from natural resources [6–8], EM harvesting is more suitable for low energy devices such as sensor networks with simple sensing tasks. Densely deployed sensor networks with low transmission distances and tolerance for long sleep cycles, during which, EH can be performed, are suitable platforms for EM harvesting. An example would be a scientific project where heat and/or humidity change of a certain region is to be monitored over the year or possibly several years. EM EH provide the required long node lifetime and the throughput requirement is rather low, because gathering heat or humidity data (a few bytes at most), say every half an hour is sufficient.

Machine to machine (M2M) communications is currently a very hot topic for the research community. The number of devices connected to the Internet is predicted to reach billions by 2020 [9]. M2M communication is considered to be the means of controlling, configuring, maintaining, and obtaining data from these devices. It will be very impractical to empower such huge number of devices by standard batteries. Furthermore, for cases like wireless sensor networks, nodes are distributed over a large area and battery replacement is not feasible most of the time. EM EH is a very promising means to provide power for such devices.

The main limiting factor in the implementation of EM EH networks is the higher power dissipation of the transceivers in reception and transmission modes compared with EH power that can be harvested. Fortunately, there are ultra low power chips that require much less power compared with conventional sensors. In [10], a wireless sensor node designed specifically for low energy applications is reported to have 61 times improvement in overall energy consumption compared with the MICA sensor for a one day run of environmental data collection. The author also mentions an on-chip receiver they are developing that only consumes 0.9 mW. Ultra-low power transceivers with similar power consumption are now commercially available. One such transceiver draws only 0.9 mA with a 1 V supply while transmitting at -6 dBm [11]. In [12], an ultra-low power transceiver which draws only 15 μA from a 15.5 V source during transmission is reported. Compared with MICA, which has a power consumption of 15 mW in receive mode, these are very promising developments.

Even though transceiver is generally the unit that has the most power consumption, other units such as the sensor itself, CPU, and RAM should also be considered. There are also very promising improvements in all of these areas. In [13], a temperature sensor that only requires 3.6 nJ to achieve a resolution of 63 mK with a conversion time of 6 ms is presented. In [14], an ultra-low power CPU that dissipates 297 nW in active mode and 29.6 pW in sleep mode is introduced. There are other similar work with similar power consumption for both sensors [15–18] and CPU [19, 20].

With potentially infinite energy, additional capabilities can be introduced to wireless devices. Opportunistic spectrum access is one of the most promising capabilities due to the increasing demand for wireless spectrum and the arising need to dynamically access it. By adding cognitive radio capability to the wireless devices, spectrum utilization can be increased [21].

Various aspects of cognitive EH networks have been analyzed in the literature. In [22], optimal times for EH and transmission is investigated based on the amount of interference on the channel. A dynamic channel selection problem in a multichannel radio frequency (RF)-powered cognitive radio network is examined in [23]. Most of the previous work assume that the EH rate is constant, or its distribution is known. Furthermore, most assume that there is a separate unit for EH on the node; thus, EH and transmission can be performed concurrently. However, the main motivation for EM EH is that existing antenna can be used as EH unit and no additional equipment is needed. Moreover, to the best of our knowledge, none of the previous work lay out an analysis of the effect of cooperation in cognitive EM EH networks.

DOI: 10.1002/dac

Even though cooperation is thoroughly investigated for conventional, battery operated wireless networks, the cost of cooperation differ between these networks, and EH wireless networks. In conventional networks, the main concern is the trade-off between the gain obtained by cooperation and the extra energy spent. In EH networks, consumed energy is not important as long as the harvesting rate is high enough to cover the power dissipation. In this regard, cooperation in EM networks is constrained by power, rather than energy.

In this paper, we provide analysis on various aspects of cognitive EM EH networks. We provide analysis on how much throughput is realistically achievable on average. Our contribution can be listed as follows:

- Contrary to most of the previous work, we do not assume exact or statistical knowledge of EH profile. Neither do we assume a separate antenna unit for EH. Assuming energy is harvested from the primary user (PU) network, we first examine the average power that can be harvested by a single secondary user (SU) node. We assume a stochastic network geometry for the PU network. We use a model that is widely used in the literature for modeling wireless node distributions, that is, Poisson point process (PPP).
- We model node operation as a Markov chain, in which, certain energy levels of the battery corresponds to states of the Markov chain. Then, we find the maximum average throughput that can be obtained for different PU channel occupation probabilities. This gives us an insight on how feasible a secondary EH harvesting network is for crowded and uncrowded spectrum cases. The trade-off is for a crowded spectrum, higher EH rates are expected. However, transmission opportunities are low. Vice verse for the uncrowded case.
- We also derive the equations for the durations of spectrum sensing, transmission and EH for achievable expected throughput.
- Then we focus on the cooperative case. We show that cooperation is not always the best choice to increase the expected throughput. We find the threshold transmission distance, when cooperation increases the expected throughput.

2. SYSTEM MODEL

We consider a 2D primary wireless network. There are N_{PU} PU nodes distributed in a circular area of radius R_{PU}, according to PPP of intensity λ. The secondary network, that is, the cognitive EM EH network is co-located with the PU network but is not necessarily limited in the same circular area. We focus our investigation on a single SU node, that is assumed to be at the origin, without loss of generality [24]. We assume that the investigated node communicates with another SU node that is at a distance d_x. We provide analysis on how this transmission distance effects the viability of cooperation.

We assume that each SU transceiver has a single antenna and can perform only one task at a time, that is, EH, spectrum sensing, transmission, or reception. The frequency range of interest is comprised of C non-overlapping contiguous channels, each with a bandwidth of B. Time is assumed to be slotted. For the transceiver and the EH units, each time slot, T, consists of three phases. The first phase is for EH and lasts for t_h. In the second phase, spectrum is sensed for s channels for a total duration of t_s. In the final phase, data transfer takes place on an available channel for t_x seconds. The CPU and the sensor units spend most of the time in sleep mode, t_{cs}, and only wake up for spectrum sensing and to take a sensor measurement and store it, which lasts for t_{ca}. The time slot structure from the transceiver and EH units and the CPU and sensor units is shown in Figure 1.

The energy harvested in the first phase plus the amount of energy inside the battery should at least be sufficient to cover energy spent in the second and third phases. We take T as constant. We calculate t_s according to spectrum sensing performance criteria and analyze how t_h and t_x should be chosen to increase expected throughput.

The amount of time spent on spectrum sensing is determined according to the spectrum sensing accuracy requirements, that is, the node is required to have a detection probability (P_d) greater than δ, even in very low signal-to-noise ratio (SNR) values such as -20 dB, to protect the PU network

DOI: 10.1002/dac

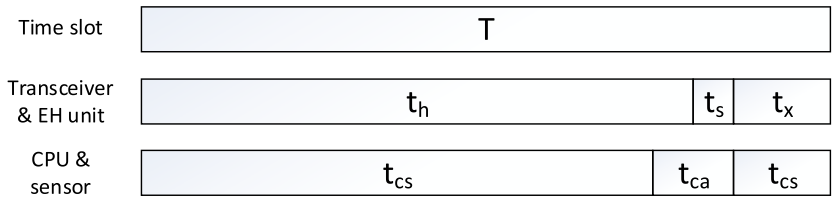

Figure 1. Time slot structure.

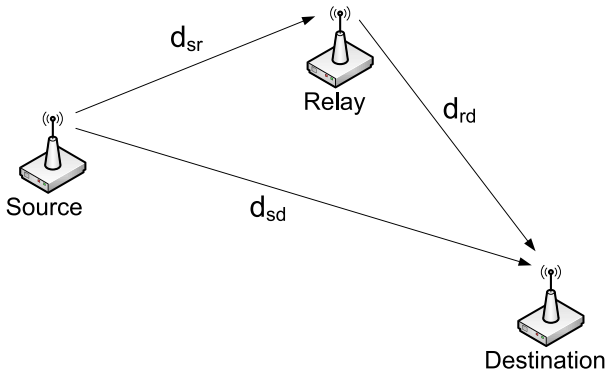

Figure 2. Structure of the cooperative relaying.

from extreme interference of SU network. Furthermore, false alarm probability (P_f) should be below β to assure a certain level of spectrum utilization.

At the beginning of a spectrum sensing phase, a channel is assumed to be busy with probability P_{PU}. Given a channel is busy, the PU that is using it may be any one of the total N_{PU} PUs with probability $1/N_{PU}$. During EH, the EM energy received from the whole band is sent to the EH unit which performs the RF to direct current conversion as well as increasing voltage with voltage multipliers to bring it to levels required to operate circuit boards. Each SU node is equipped with a battery that is charged by this EH unit.

In the cooperative case, the time slot is divided into four phases. First, phase is EH. Then, all nodes perform spectrum sensing in a cooperative manner. Overall spectrum sensing decision is made by an OR fusion rule, where logical or operation is performed on sensor decisions to make the final decision. Each node sends its individual spectrum sensing result, and PU existence is decided if one or more of the nodes detect PU. Complex spectrum management schemes are out of the context of this paper. We assume that each node sends its results in a single bit to others by taking turns in a pre-arranged manner through a control channel. For data transmission, cooperating nodes act as relays as shown in Figure 2. In the third phase, the source node transmits its data and the destination node and cooperating nodes, acting as a relays, receive this data. Final phase is the relaying phase in which relay nodes take turns to transmit the data to the destination.

We assume fading to be as in [25, 26], that is, channel gains are affected by both small-scale fading and large-scale path loss; however, amount of received power is dominated by the path loss [27, 28]. Under this model, fading power is an exponential random variable with unit variance. The path loss is proportional to $d^{-\alpha}$, where d is the Euclidean distance and $\alpha > 2$ is the path loss exponent.

3. ANALYSIS OF NON-COOPERATIVE COMMUNICATION

We aim to determine the maximum expected throughput, Γ, in a cognitive EH harvesting network.

$$\max \Gamma = R(P_d, P_f, t_s, t_x, P_x, E_i) \cdot t_x / T \tag{1}$$

s. t.

DOI: 10.1002/dac

$$P_d \geqslant \delta \tag{2}$$

$$P_f \leqslant \alpha \tag{3}$$

$$T = t_s + t_h + t_x \tag{4}$$

$$E_i + E_h \geqslant E_{cs} + E_x + E_s \tag{5}$$

where R is the optimal transmission rate that maximizes throughput, P_x is the corresponding optimal transmission power, E_i is the amount of energy that is left in the battery from the previous time slot, and E_h is the harvested energy. E_{cs} is the amount of energy dissipated by the CPU and the sensor. The first two constraints are related to spectrum sensing. The third constraint is about the periodic time slot operation. The final constraint is the energy causality constraint. It is to make sure we do not try to spend more energy than we have.

Our approach in solving Equation (1) is to first determine the sensing time, t_s, using the constraints (2) and (3). Then, for a given E_i, the problem reduces to finding the optimal trade off between t_x and P_x. If we increase t_x, time left for harvesting reduces, and thus, P_x reduces. If we decrease t_x, EH time, and thus, harvested energy increases. Therefore, P_x increases. However, time left for communication, t_x, is now much lower, which reduces the throughput. We detail how we solve this problem in Section 3.3.

To sum up, we seek the answers of the following questions to find the solution to Equation (1),

(1) What should be the spectrum sensing time for one channel to meet $P_f \leqslant \beta$ and $P_d \geqslant \delta$ for minimum SNR, that is, γ_{min}?
(2) What is the expected amount of power that can be harvested under these conditions?
(3) What should be the transmission time and the transmission power to obtain achievable expected throughput under these conditions?

We lay out the answers in the following analysis.

3.1. Spectrum sensing time

The detection and false alarm probabilities for a single node performing sensing on an AWGN channel is given as [29]

$$P_d = Q\left(\frac{\zeta - N\left(\sigma_n^2 + \sigma_s^2\right)}{\sqrt{2N}\left(\sigma_n^2 + \sigma_s^2\right)}\right) \tag{6}$$

$$P_f = Q\left(\frac{\zeta - N\sigma_n^2}{\sqrt{2N}\sigma_n^2}\right) \tag{7}$$

where ζ is the detection threshold, N is the number of required samples, σ_s^2 and σ_n^2 are the signal and noise power, respectively. $Q(\cdot)$ is the q-function, that is, $Q(x) = 1/2\pi \int_x^\infty exp(-u^2/2)\mathrm{d}u$.

The detection threshold, ζ, that satisfies $P_d \geqslant \delta$, can be found by replacing P_d with δ in Equation (6), and solving for ζ,

$$\zeta = Q^{-1}(\delta)\sqrt{2N}\left(\sigma_n^2 + \sigma_s^2\right) + N\left(\sigma_n^2 + \sigma_s^2\right) \tag{8}$$

To find the required number of samples to meet $P_d \geqslant \delta$ under γ_{min}, we substitute (8) in (7). Assuming the sampling rate is equal to the Nyquist rate, after algebraic manipulations, we obtain the required spectrum sensing time for one channel,

$$t_{s1} = \frac{1}{B}\left(\frac{Q^{-1}(\beta) - (1+\gamma_{min})Q^{-1}(\delta)}{\gamma_{min}}\right)^2 \tag{9}$$

DOI: 10.1002/dac

where B is the channel bandwidth. Note that bandwidth is inversely proportional to the spectrum sensing duration. Therefore, as the channel bandwidth decreases, spectrum sensing time increases. In fact, when channel bandwidth is lower than a threshold value, t_s may increase so much that there isn't enough harvesting time and transmission becomes impossible.

This is shown in Figure 3, where the continuous line is the energy spent on spectrum sensing for various channel bandwidth values and the dotted line is the amount of energy that can be harvested in the remaining time. At around 9 KHz bandwidth, spectrum sensing consumes all of the harvested energy and no transmission can be performed. As the bandwidth goes lower, the harvested energy cannot even cover the spectrum sensing phase. As seen here, for a system with specs given in Table I, bandwidth should be higher than 9 KHz. An alternative is to use compressive sensing and use sub-Nyquist samples. However, we note that compressive sensing requires sparsity and is more suitable for mostly vacant spectrum, which is not very fitting for EH networks.

Unless otherwise stated, we use the typical values given in Table I for this and all of the following figures. Node density, energy consumption calculations, loss model, and as a result, EH profile are all determined according to these values. Nodes are deployed according to PPP distribution, as detailed in Section 2. Power dissipation values are chosen as in the related references. We assume

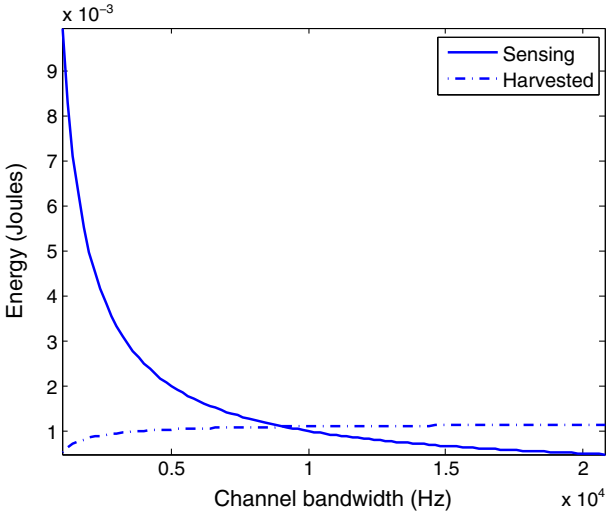

Figure 3. Harvested energy and energy spent on sensing.

Table I. Typical parameter values.

Parameter	Meaning	Value
Typical parameter valuesB	Bandwidth	200 KHz
R	Radius of PU network area	35 m
T	Time slot duration	120 s
δ	Required detection prob.	0.9
β	Required false alarm prob.	0.1
α	Path loss exponent	3.4
γ_{min}	Minimum SNR	−20 dB
P_t	PU transmission power	250 mW
d_x	Transmission distance	35 m
V	Sensor supply voltage	1.55 V [12]
I_s	Current drawn in sensing mode	15 μA [12]
P_{ca}	Active power dissptd. by CPU	297 nW [14]
t_{ca}	Time CPU spent in active mode	18.8 ms [14]
P_{cs}	Passive power dissptd. by CPU	29,6 pW [14]
E_{sa}	Energy dissipated by the sensor	3.6 nJ [13]

DOI: 10.1002/dac

execution of 2,000 instructions is required to take one sensor measurement as used in [14]. With a 106 KHz CPU as in [14], this corresponds to an approximate active duration of $t_{ca} = 18.8$ ms.

PU transmission power is chosen as 250 mW. This is half of the maximum allowed transmission power for power class 2 UEs [30]. Taking into account the power control mechanism, we didn't use the maximum allowable power. Taking an even lower transmission power would mean that the base station is nearby, and it is possible to harvest energy from it. While this is also a possible case, we took the worse case by not assuming a nearby base station.

In IEEE 802.22 standard, DTV protection at -114 dBm corresponds to an SNR of -19 dB for equivalent receiver noise figure of 11 dB and 22 dB safety margin at edge of coverage [31]. We took minimum SNR as -20dB. Also, minimum detection probability of $\delta = 0.9$, and maximum false alarm probability of $\beta = 0.1$ is required.

The radius of the PU network is taken as 35 m. Because of practical considerations, a certain minimum received power is required for EH to be possible. As an example, in [32] a minimum of -22 dBm is reported as minimum received RF power requirement. Using our channel model and a PU transmission power of 250 mW, 34 m is the maximum distance from which -22 dBm power can be received.

3.2. Harvested power

The average harvested power can be written as $E[P_h] = \sum_{p=1}^{N_{PU}} \eta_{eh} E_p[P_r] P_p$, where η_{eh} is the harvesting efficiency, $E_p[P_r]$ is the expected received power when p PUs are active, P_r is the received power, and P_p is the probability of having p PUs active. P_p can be written as $P_p = P_{PU}^p (1 - P_{PU})^{(N_{PU}-p)} \binom{N_{PU}}{p}$.

To find $E_p[P_r]$, we form a list, $\mathcal{P}$, of the PUs, in the order of their distance to the investigated EH node. When PUs have a PPP distribution, the density function of the distance (d_n) between the n^{th} PU in $\mathcal{P}$ and the EH node is given by [24]

$$f_{d_n}(r) = e^{-\lambda \pi r^2} \frac{2(\lambda \pi r^2)^n}{r \Gamma(n)}, \quad r \in \mathbb{R} \tag{10}$$

where $\Gamma(\cdot)$ is the Gamma function. The expected value of the distance to the n^{th} closest neighbor can be expressed as [24]

$$E[d_n] = R \sqrt{\frac{n}{N_{PU} + 1}} \tag{11}$$

Furthermore, let $\mathcal{A}_p$ be the set that consists of p combinations of PUs in $\mathcal{P}$, and $|\mathcal{A}_p|$ be the size of the set. Then,

$$E_p[P_r] = \frac{1}{|\mathcal{A}_p|} \sum_{k=1}^{|\mathcal{A}_p|} \sum_{n \in \mathcal{A}_p} P_t E[d_n]^{-\alpha} \tag{12}$$

The inner sum is the combined received energy when a certain p-combination of PUs are active. Because all PUs have the same probability to be active, all p-combinations are equally probable for a given p. Therefore, average over all possible p-combinations gives the expected received power when p PUs are active. Combining all,

$$\begin{aligned} E[P_h] = \sum_{p=1}^{N_{PU}} \frac{1}{|\mathcal{A}_p|} \sum_{k=1}^{|\mathcal{A}_p|} \sum_{n \in \mathcal{A}_p} P_t R^{-\alpha} \left(\frac{n}{N_{PU} + 1} \right)^{-\alpha/2} \\ \eta_{eh} P_{PU}^p (1 - P_{PU})^{(N_{PU}-p)} \binom{N_{PU}}{p} \end{aligned} \tag{13}$$

DOI: 10.1002/dac

3.3. Maximum expected throughput

Node operation in a time slot, T, begins with EH, then spectrum is sensed and finally transmission takes place. However, sometimes an available channel may not be found and the harvested energy remains in the battery, ready to be utilized in the next time slot. Throughput calculations should take this into account. To achieve this, we model the node operation as a Markov chain, where each state corresponds to the amount of energy remaining in the battery from the previous time slot. If the amount of energy in the battery remaining from the last time slot is not sufficient to supply one environment and spectrum sensing phase, the system is in state 0. If remaining energy is sufficient to cover one environment and spectrum sensing phase, but not two sensing phases, the system is in state 1 and so on. Our Markov chain model is depicted in Figure 4. If we find an available channel, we spend the remaining energy in transmission and go to state 0. If no available channel is found, there are three possibilities. If the harvested energy is not sufficient to cover the sensing tasks (i.e. environment and spectrum sensing) in that slot, we move down one state. If it is only sufficient to cover sensing in that slot, we stay in at the same state. Otherwise, we move to one of the higher states.

Associated transition probabilities are written in terms of:

P_a: Pr(at least one available channel decided in n channel senses)$= 1 - (P_{PU}P_d + (1 - P_{PU})P_f)^n$

P_0: Pr(harvested energy is not sufficient for even one sensing phase) $= Pr(E[P_h] < E_{s1})$

P_i: Pr(harvested energy is sufficient for i sensing phases but not $i + 1$) $= Pr(E_{si} \leqslant E[P_h] < E_{s(i+1)})$

$P_{>k}$: Pr(harvested energy is sufficient to cover more than k sensing phases) $= Pr(E[P_h] \geqslant E_{sk})$

In calculation of P_a, we take into account two cases. Either PU is active and we detect it, or there is no active PU but sensing raises a false alarm. E_{si}, is the amount of energy consumed in i spectrum sensing phases.

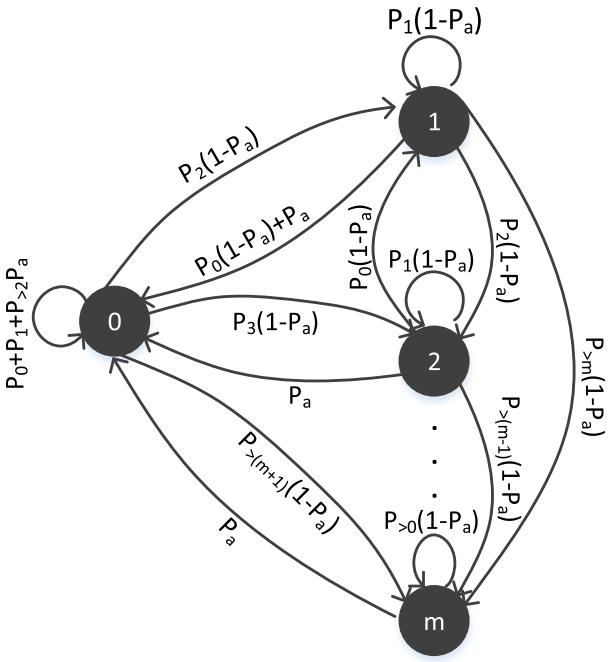

Figure 4. Markov modeling of node operation.

DOI: 10.1002/dac

The maximum throughput can be written as AWGN channel capacity times the ratio of time spent in transmission to the time slot duration when moving from state i to state j.

$$\Gamma = \sum_{i=0}^{m}\sum_{j=0}^{m} B\log_2\left(1+\frac{\eta_x d_x^{-\alpha} P_x(i,j)}{P_n}\right)\frac{t_x(i,j)}{T}\pi_i S(i,j) \tag{14}$$

where d_x is the transmission distance, α is the path loss exponent, $\pi_0 \cdots \pi_m$ are the steady state probabilities of the Markov chain, and $S(i,j)$ are the state transition probabilities for moving from state i to state j. The state transition matrix is given in (15). The actual amount of power transmitted as RF power depends on the transmitter efficiency. A transmitter radiates $\eta_x P_x(i,j)$ amount of power when operation moves from state i to state j.

$$S(i,j) = \begin{bmatrix} P_0+P_1+P_{>2}P_a & P_2(1-P_a) & P_3(1-P_a) & \cdots & P_{>(m+1)}(1-P_a) \\ P_0(1-P_a)+P_a & P_1(1-P_a) & P_2(1-P_a) & \cdots & P_{>m}(1-P_a) \\ P_a & P_0(1-P_a) & P_1(1-P_a) & \cdots & P_{>(m-1)}(1-P_a) \\ \vdots & \vdots & \vdots & \ddots & \vdots \\ P_a & 0 & \cdots & P_0(1-P_a) & P_{>0}(1-P_a) \end{bmatrix} \tag{15}$$

There is a trade-off between the choice of transmission time, t_x, and transmission power, P_x. If t_x is chosen as a long duration, the amount of transmitted data increases. However, because the overall time slot duration, T, is fixed, increasing t_x causes EH time, t_h, to be lower. With lower energy at hand, P_x is reduced, which causes the transmission rate to drop. This is shown in Figure 5. When P_x is too low, throughput is low. As P_x is increased throughput begins to increase. However, as P_x increases, t_x must decrease so that the energy causality relation $E_i + P_h t_h \geq E_{cs} + P_x t_x + P_s t_s$ holds. Here, E_{cs}, that is, the energy spent by CPU and the sensor can be written as

$$E_{cs} = E_{sa} + P_{ca}t_{ca} + P_{cs}(T - t_{ca}) \tag{16}$$

where E_{sa} is the energy spent by the sensor to get one reading, P_{ca} and t_{ca} are the power dissipated and time spent by the CPU in active mode, respectively. P_{cs} is the power used by the CPU in sleep mode. Because the CPU is in sleep after taking the reading, the time spent in sleep mode by the CPU is rest of the slot time, that is, $T - t_{ca}$. Checking (14), we see that t_x is a linear factor of throughput and P_x is inside the logarithm. Due to the nature of energy causality and throughput equations, decreasing P_x and increasing t_x causes throughput to increase faster.

We see that without cooperation, throughput up to about 60 bps can be achieved. This means, for a time slot of 120 s, about 720 bytes can be sent at each time slot, which should be sufficient for most simple sensing applications.

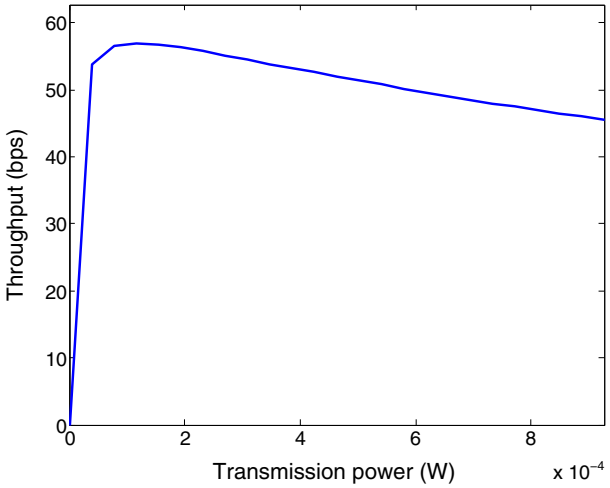

Figure 5. Throughput versus transmision power when energy is harvested from EM waves.

DOI: 10.1002/dac

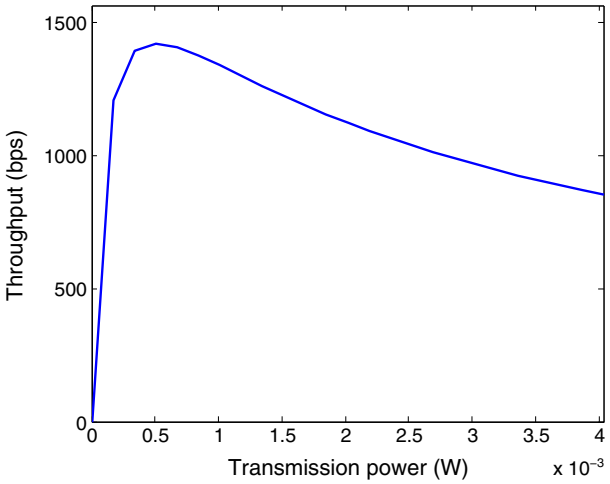

Figure 6. Throughput versus transmission power when energy is harvested from ambient light.

To have a comparison with alternative EH schemes, in Figure 6, we provide the throughput if a 1 cm^2 solar panel was used to harvest energy from indoors ambient light instead of harvesting energy from EM waves. As stated in [33], we use an average harvested power of 10 $\mu W/cm^2$. We see that considerable improvement is possible. However, we should keep in mind that harvesting energy from light sources requires additional equipment on the nodes, that is, solar panels, and enforces restrictions on node placement, that is, the sensor must be placed out in the open to be able to harvest energy. Furthermore, it is only possible as long as the environment is illuminated.

Next, we try to find a tractable solution for the optimal value of P_x. We first note that $t_x = T - t_s - t_h$, and $E_i + P_h t_h = E_{cs} + P_s t_s + P_x t_x$. Then we place these expressions into (14), take the derivative with respect to P_x and equate to zero.

$$\frac{d\Gamma}{dP_x} = \frac{B\left[P_h - ((P_h + P_s)t_s - E_i + E_{cs})/T\right] d_x^{-\alpha}\eta_x}{P_n(P_x + P_h)\left(1 + \frac{P_x d_x^{-\alpha}}{P_n}\right)\ln 2} - \frac{B\left[P_h - ((P_h + P_s)t_s - E_i + E_{cs})/T\right]\ln\left(1 + \frac{Px d_x^{-\alpha}}{P_n}\right)}{(P_x + P_h)^2 \ln 2} = 0 \tag{17}$$

which yields

$$P_x = \left[\frac{\frac{P_h d_x^{-\alpha}\eta_x}{P_n} - 1}{\frac{\eta_x d_x^{-\alpha}}{P_n} L\left(\frac{P_h d_x^{-\alpha}\eta_x}{eP_n} - \frac{1}{e}\right)} - 1\right]\frac{P_n}{d_x^{-\alpha}\eta_x} \tag{18}$$

where L is the Lambert W function, that is, for any complex number z, the defining function of $L(z)$ is $z = L(z)e^{L(z)}$. We present the details of the derivations of (17) and (18) in the Appendix.

Using (18) in (14), we obtain the maximum achievable throughput. In Figure 7, we depict optimal transmission power for various PU existence probabilities. When PU existence probability, P_{PU}, is too low, the harvested energy is also too low. As P_{PU} increases, harvested energy increases and transmission power also increases. As P_{PU} keeps increasing, it becomes better to reduce P_x and increase t_x. This was depicted in Figure 5. Therefore, optimal power reduces as P_{PU} keeps increasing.

In Figure 8, we show the impact of PU existence probability and PU network node density on energy harvesting and thus on throughput. Radius of the network is changed while the number of PUs inside remain the same, that is, 10 PUs. As the radius increases, the average distance of PUs from the investigated SU node increases. As a result, average harvested power decreases. This causes throughput to decrease. As for the PU existence probability, when this probability is low,

DOI: 10.1002/dac

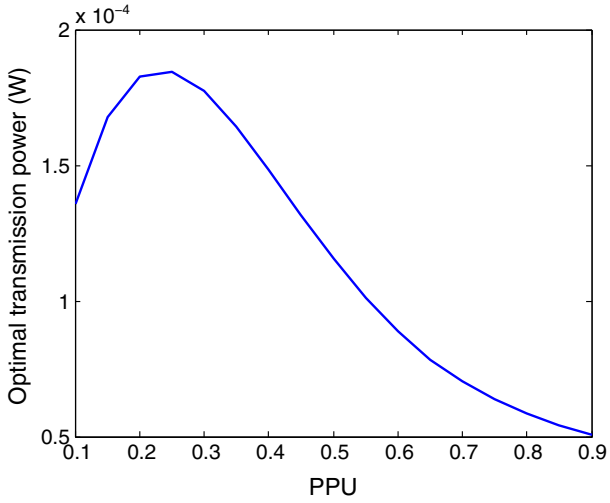

Figure 7. Optimal transmit mode power versus primary user (PU) existence probability.

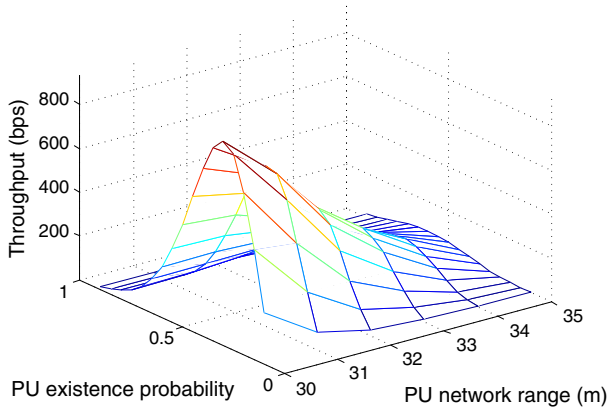

Figure 8. Achievable expected throughput for varying harvesting time and primary user (PU) existence probability.

harvested energy is low because there are not many active PUs. As it increases, harvested energy and thus, throughput increases. However, after a certain probability, even though the harvested energy increases, probability of finding an available channel decreases. Because transmission is halted to the next time slot in such cases, throughput begins to drop.

This suggests that the proximity of PUs is extremely important for EM EH networks, and also, the sweet spot is when the PUs are active about half of the time to enable effective EH and also provide opportunity for transmission.

4. ANALYSIS OF COOPERATIVE COMMUNICATION

Our aim is the same as the non-cooperative case, that is, to find the maximum achievable throughput. We focus on a network with two cooperating nodes. Extension to more cooperating nodes is straightforward. We assume there is no change in EH conditions of the previous section to be able to make a fair comparison. In the spectrum sensing phase, the overall detection (Q_d) and false alarm probabilities (Q_f) under OR fusion rule are given as

$$Q_d = 1 - (1 - P_d)^n \tag{19}$$

$$Q_f = 1 - (1 - P_f)^n \tag{20}$$

DOI: 10.1002/dac

where n is the number of cooperating users. Therefore, in this case, we have $Q_d \geq \delta$ and $Q_{fa} \leq \beta$ as spectrum sensing requirements.

The required sensing duration for one channel can be obtained by taking similar steps used in derivation of Equation (9)

$$t_{s1} = \frac{1}{B}\left(\frac{Q^{-1}(\Theta) - (1+\gamma_{min})\,Q^{-1}(\Delta)}{\gamma_{min}}\right)^2 \tag{21}$$

where $\Theta = 1 - \sqrt{1-\beta}$ and $\Delta = 1 - \sqrt{1-\delta}$ for two node cooperation. In Figure 9, we depict the harvested energy and the amount of energy spent in spectrum sensing for various channel bandwidth values. Comparing with Figure 3, we see that cooperative case allows use of lower bandwidth, where the breakeven point has moved from about 9 KHz to 6 KHz. Because in cooperative sensing, each individual node has to meet more relaxed sensing requirements, (P_d is always lower than Q_d, etc.), number of required samples is lower. This enables a lower minimum bandwidth to be viable.

In cooperative relay-based communication, the destination node receives the signal from both the source and the relay. Two prominent relaying methods are amplify and forward (AF) and decode and forward (DF). For the DF case, we assume that the relay node can successfully decode the data if SNR is above a modulation dependent threshold value [34]. SNR at the destination for these two cases is

$$\gamma_{AF} = \frac{P_x\left(\eta_x d_x^{-\alpha} + \frac{P_x \eta_x^2 d_r^{-2\alpha}}{P_x \eta_x d_x^{-\alpha} + P_n}\right)}{P_n\left(1 + \frac{P_x \eta_x d_r^{-\alpha}}{P_x \eta_x d_x^{-\alpha} + P_n}\right)} \tag{22}$$

$$\gamma_{DF} = \frac{P_x(\eta_x d_x^{-\alpha} + \eta_x d_r^{-\alpha})}{P_n} \tag{23}$$

Throughput expression for the cooperative case is the same as Equation (14). However, calculation of $P_x(i,j)$ and $t_x(i,j)$ differ, because the required sensing time is reduced in cooperative sensing. Like the non-cooperative case, there is a trade-off between t_x and P_x. We can simplify the analysis by writing one in terms of the other. Note that $T = t_h + t_s + t_r + t_x$, where t_r is the receiving duration for the relay and $t_r = t_x$. Also note that $E_i + P_h t_h = E_{cs} + P_s t_s + P_r t_r + P_x t_x$ due to energy causality requirement and $P_r = P_s$ because both are power consumed in receive mode. Using these equations, t_x can be written in terms of P_x and known identities P_h, P_s, T, t_s.

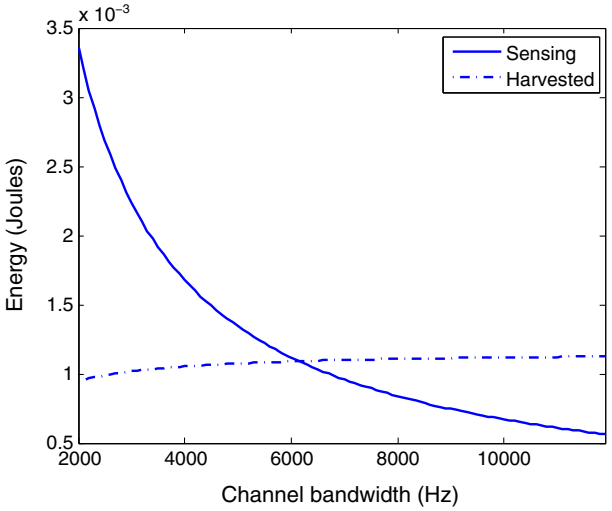

Figure 9. Harvested energy and energy spent on sensing for cooperative sensing.

DOI: 10.1002/dac

Using the SNR expressions (22) and (23), the maximum expected throughput for AF and DF cases can be written as,

$$\Gamma_{AF} = \frac{1}{B}\log_2\left(\frac{P_x\left(\eta_x d_x^{-\alpha} + \frac{P_x\eta_x^2 d_r^{-2\alpha}}{P_x\eta_x d_x^{-\alpha}+P_n}\right)}{P_n\left(1+\frac{P_x\eta_x d_r^{-\alpha}}{P_x\eta_x d_x^{-\alpha}+P_n}\right)}\right)\frac{P_h-(E_{cs}-E_i+(P_h+P_s)t_s)/T}{P_x+2P_h+P_s} \tag{24}$$

$$\Gamma_{DF} = \frac{1}{B}\log_2\left(\frac{P_x(\eta_x d_x^{-\alpha}+\eta_x d_r^{-\alpha})}{P_n}\right)\frac{P_h-(E_{cs}-E_i+(P_h+P_s)t_s)/T}{P_x+2P_h+P_s} \tag{25}$$

Throughput for varying P_x is shown in Figure 10. Behavior is the same as the non-cooperative case as expected. Similar to the approach in the non-cooperative case, the achievable expected throughput can be calculated by differentiating (24) and (25) with respect to P_x, equating to zero to find P_x, then substituting it back into the equations. Unfortunately, (24) is too complex to find a closed form expression for P_x. However, for the DF case, P_x can be found using similar steps in derivation of (18) as detailed in the Appendix.

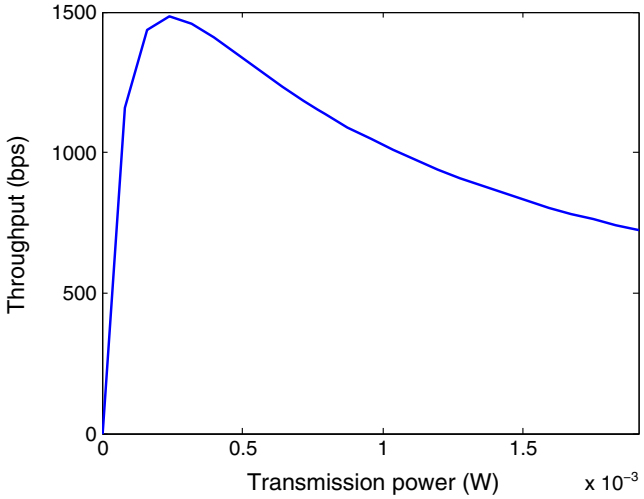

Figure 10. Throughput versus transmission power.

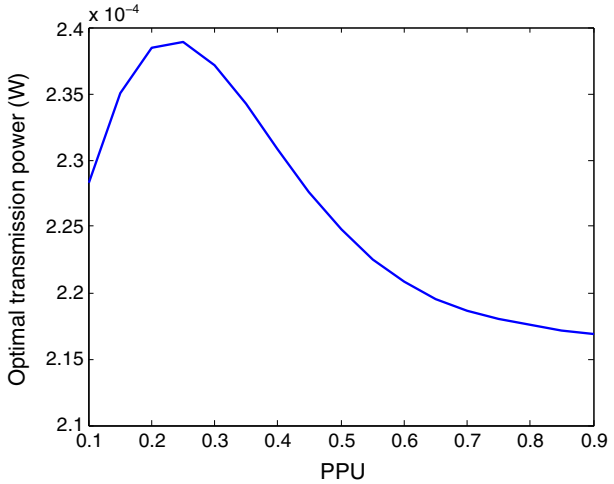

Figure 11. Optimal transmit mode power versus primary user (PU) existence probability for decode and forward.

DOI: 10.1002/dac

$$P_x = \left[\frac{W(2P_h + P_s) - 1}{WL\left(\frac{W}{e}(2P_h + P_s) - \frac{1}{e}\right)} - 1 \right] \frac{1}{W} \tag{26}$$

where $W = \frac{\eta_x (d_{sd}^{-\alpha} + d_{rd}^{-\alpha})}{P_n}$. Here, d_{sd} is the distance between source and destination nodes and d_{rd} is the destination between relay and destination nodes. We plot the optimal transmission power for various spectrum occupancy rates in Figure 11. We see that higher transmission power can be used for the cooperative case. The reason is that nodes spend less energy in spectrum sensing and they can use the remaining energy for higher transmission power.

In Figure 12, we show how maximum expected throughput changes with PU existence probability and PU network radius. Comparing Figure 12 with Figure 8, we see that cooperation, indeed,

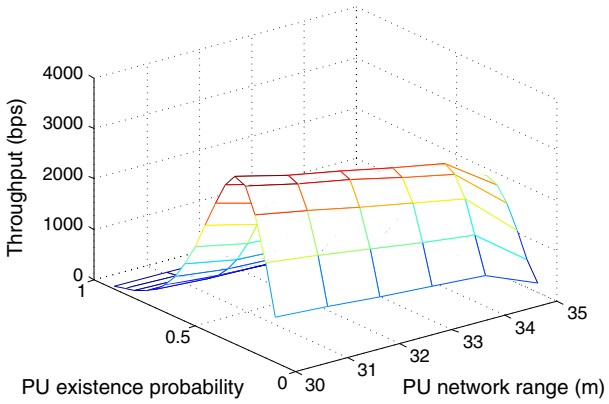

Figure 12. Achievable expected throughput for varying harvesting time and primary user (PU) existence probability for decode and forward.

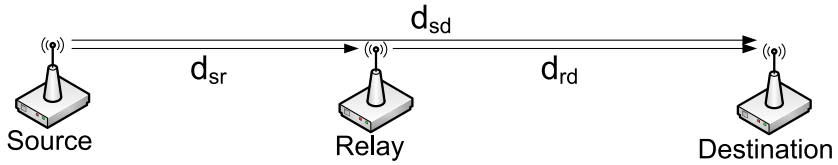

Figure 13. Best case node placement for relaying.

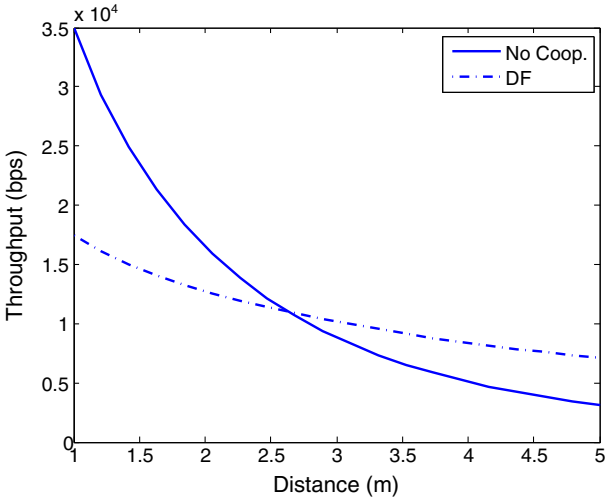

Figure 14. Achievable throughput versus transmission distance.

DOI: 10.1002/dac

increases the throughput. However, does this hold for all transmission distances? We expect cooperation to yield poor results when the transmission distance is low, that is, when the overhead of cooperation is not worth its benefit. We want to find the conditions under which relaying, together with cooperative spectrum sensing increases the expected achievable throughput. We try to find the cases for which cooperation is not viable even for the best case node placement scenario. By best case node placement, we mean the case where the source, relay, and destination are on the same line and relay is between the source and the destination. For the DF case, the best placement is when d_{sr} is such that SNR at the relay is equal to the decoding threshold, where it will be as close to the destination while still being able to decode the data from the source. We depict this in Figure 13.

In Figure 14, we plot achievable throughput versus transmission distance, using optimal P_x values obtained by Equations (18) and (26) for the non-cooperative and DF cases, respectively. As seen here, for the typical values given in Table I, cooperation yields worse results only if communication distance is really low, that is, lower than 2.5 m. This suggests that, unless the SU sensor network is extremely densely deployed, cooperation should be used.

5. CONCLUSIONS

We present an analysis of expected maximum throughput in EM EH CRSN. Instead of assuming the exact or statistical EH profile knowledge, we derive the expected harvested energy by investigating a common wireless network topology where PUs, from which the EM energy is harvested, are located according to a PPP process. We emphasize some parameters that must be paid attention to, especially in EH. One such parameter is the channel bandwidth and its effect on spectrum sensing time. We point out that when Nyquist sampling rate is used, higher sensing time is required for lower bandwidth. This puts a lower limit on the PU channel bandwidth that can be utilized. We show this break even point, where the harvested energy is equal to the energy spent in spectrum sensing.

Overall, our results indicate that EM EH is feasible for a cognitive wireless sensor network if it can tolerate high sleep cycles. It is worth noting that the maximum throughput depends on the PU existence probability. Therefore, our scheme could be improved by a learning algorithm which can keep track of PU activities. Another method is to use cooperation in spectrum sensing and relaying in data transmission, because this reduces the power required by each node. We examine the cooperative case and provide the solution for maximum expected achievable throughput for DF. Then, we point out the fact that cooperation may not always be the better solution, and we investigate the condition under which cooperation yields higher expected throughput.

APPENDIX

Throughput can be written as

$$\Gamma = B \log_2 \left(1 + \frac{d_x^{-\alpha} \eta_x}{P_n} P_x\right) \frac{t_x}{T} \tag{A.1}$$

where

$$E_i + P_h t_h = E_{cs} + P_s t_s P_x t_x \tag{A.2}$$

and

$$t_h = T - t_s - t_x \tag{A.3}$$

Therefore, t_x / T can be written as

$$\frac{t_x}{T} = \frac{E_i + P_h T - P_h t_s - P_s t_s - E_{cs}}{T(P_x + P_h)} \tag{A.4}$$

$$= \frac{P_h - [(P_h + P_s)t_s - E_i + E_{cs}]/T}{P_x + P_h} \tag{A.5}$$

DOI: 10.1002/dac

Let

$$A = \frac{\eta_x d_x^{-\alpha}}{P_n} \tag{A.6}$$

$$C = P_h - [(P_h + P_s)t_s - E_i + E_{cs}]/T \tag{A.7}$$

$$D = P_h \tag{A.8}$$

$$x = P_x \tag{A.9}$$

so that throughput can be simplified in notation as

$$\Gamma = B \log_2(1 + Ax)\frac{C}{x + D} \tag{A.10}$$

Then

$$\frac{d\Gamma}{dx} = \frac{ABC}{\ln(2)(1 + Ax)(x + D)} - \frac{BC \ln(1 + Ax)}{\ln(2)(x + D)^2} \tag{A.11}$$

which yields (17) when values are substituted. Equating to zero and canceling common terms at each side,

$$\frac{A}{1 + Ax} = \frac{\ln(1 + Ax)}{x + D} \tag{A.12}$$

$$A(x + D) = (1 + Ax)\ln(1 + Ax) \tag{A.13}$$

$$Ax + AD - 1 + 1 = (1 + Ax)\ln(1 + Ax) \tag{A.14}$$

$$(AD - 1) + (1 + Ax) = (1 + Ax)\ln(1 + Ax) \tag{A.15}$$

$$\frac{AD - 1}{1 + Ax} + 1 = \ln(1 + Ax) \tag{A.16}$$

$$e^{(AD-1)/(1+Ax)} = \frac{1 + Ax}{e} \tag{A.17}$$

$$\frac{AD - 1}{1 + Ax} e^{\frac{AD-1}{1+Ax}} = \frac{AD - 1}{e} \tag{A.18}$$

We use the Lambert W function, defined as $z = L(z)e^{L(z)}$. For our case $L(z) = \frac{AD-1}{1+Ax}$ and $z = \frac{AD-1}{e}$. Then

$$\frac{AD - 1}{1 + Ax} = L\left(\frac{AD - 1}{e}\right) \tag{A.19}$$

$$x = \frac{AD - 1}{A\, L\left(\frac{AD-1}{e}\right)} - \frac{1}{A} \tag{A.20}$$

Substituting values of A and D, we obtain (18).

DOI: 10.1002/dac

ACKNOWLEDGEMENTS

This work was supported in part by the Turkish Scientific and Technical Research Council (TUBITAK) under grant. #110E249.

REFERENCES

1. Ozel O, Tutuncuoglu K, Yang J, Ulukus S, Yener A. Transmission with energy harvesting nodes in fading wireless channles: optimal policies. *IEEE Journal on Selected Areas in Communications* 2011; **29**:1732–1743.
2. Ho CK, Zhang R. Optimal energy allocation for wireless communications with energy harvesting constraints. *IEEE Transactions on Signal Processing* 2012; **60**(9):4808–4818.
3. Orhan O, Gunduz D, Erkip E. Throughput maximization for an energy harvesting communication system with processing cost. *Proceedings of the 2012 Information Theory Workshop*, Lausanne, Switzerland; 84–88.
4. Jeon J, Ephremides E. The stability region of random multiple access under stochastic energy harvesting. *Proceedings of the 2011 IEEE International Symposium on Information Theory*, Saint Petersburg, Russia; 1796-1800.
5. Krikidis I, Charalambous T, Thompson JS. Stability analysis and power optimization for energy harvesting cooperative networks. *IEEE Signal Processing Letters* 2012; **19**:20–23.
6. Vullers RJM, Schaijk RV, Doms I, Hoof CV, Mertens R. Micropower energy harvesting. *Elsevier Solid-State Circuits* 2009; **53**(7):684–693.
7. Bouchouicha D, Dupont F, Latrach M, Ventura L. Ambient RF energy harvesting. *Proceedings of the 2010 International Conference on Renewable Energies and Power Quality*, Granada, Spain.
8. Jabbar H, Song YS, Jeong TT. RF energy harvesting system and circuits for charging of mobile devices. *IEEE Transactions Consumer Electron* 2010; **56**(1):247–253.
9. Mason Analysys. *M2M Device Connections, Revenue and ARPU: Worldwide Forecast 20112021*, 2012.
10. Hill J L. System architecture for wireless sensor networks. *Doctor of Philosophy Thesis*, University of California, Berkeley, USA, 2003.
11. IMEC International. Available from: http://www2.imec.be/be_en/research/wireless-communication/ultralow-power-wireless-communic.html (accessed November 26, 2015).
12. Lu J, Okada H, Itoh T, Harada T, Maeda R. Toward the world amallest wireless sensor nodes with ultralow power consumption. *IEEE Sensors Journal* 2014; **14**(6):2035–2041.
13. Souri K, Chae Y, Thus F, Makinwa K. 12.7 A 0.85V 600nW all-CMOS temperature sensor with an inaccuracy of $\pm\mathbf{0.4}^{\circ}$C (3σ) from -40 to 125°C. *Proceedings IEEE International Solid-State Circuits Conference Digest of Technical Papers (ISSCC 2014)*, San Francisco, CA, USA, February 2014; 222–223.
14. Seok M, Hanson S, Lin YS, Foo Z, Kim D, Lee Y, Liu N, Sylvester D, Blaauw D. The Phoenix processor: a 30pW platform for sensor applications. *Proceedings. IEEE Symposium on VLSI Circuits*, Honolulu, HI, USA, June 2008; 188–189.
15. Souri K, Chae Y, Makinwa KAA. A CMOS temperature sensor with a voltage-calibrated inaccuracy of $\pm\mathbf{0.15}^{\circ}$C (3σ) from -55 to 125°C. *IEEE Journal of Solid-State Circuits* 2013; **47**(12):292–301.
16. Law M, Bermak A, Luong H. A sub-W embedded CMOS temperature sensor for RFID food monitoring application. *IEEE Journal of Solid-State Circuits* 2010; **45**(6):1246–1255.
17. Lin YS, Sylvester D, Blaauw D. An ultra low power 1V, 220nW temperature sensor for passive wireless applications. *Proceedings of the IEEE Custom Integrated Circuits Conference,* San Jose, CA, USA, September 2008; 507–510.
18. Wu CK, Chan WS, Lin TH. A 80kS/s 36W resistor-based temperature sensor using BGR-free SAR ADC with a unevenly-weighted resistor string in 0.18m CMOS. *Proceedings Symposium on VLSI Circuits (VLSIC 2011)*, Kyoto, Japan, June 2011; 222–223.
19. Zhai B, Nazhandali L, Olson J, Reeves A, Minuth M, Helfand R, Pant S, Blaauw D, Austin T. A 2.60pJ/Inst Subthreshold Sensor Processor for Optimal Energy Efficiency. *Proceedings Symposium on VLSI Circuits*, Honolulu, HI, USA, 2006; 154–155.
20. Hanson S, Zhai B, Seok M, Cline B, Zhou K, Singhal M, Minuth M, Olson J, Nazhandali L, Austin T, Sylvester D, Blaauw D. Performance and variation optimization strategies in a sub-200mV, 3.pJ/inst, 11nW subthreshold processor. *Proceedings Symposium on VLSI circuits*, Kyoto, Japan, 2007; 152–153.
21. Akan OB, Karli OB, Ergul O. Cognitive radio sensor networks. *IEEE Network Magazine* 2009; **23**(4):34–40.
22. Liu L, Zhang R, Chua KC. Wireless information transfer with opportunistic energy harvesting. *IEEE Transactions on Wireless Communications* 2013; **12**(1):288–300.
23. Lu X, Wang P, Niyato D, Hossain E. Dynamic spectrum access in cognitive radio networks with RF energy harvesting. *IEEE Wireless Communications* 2014; **21**(3):102–110.
24. Srinivasa S, Haenggi M. Distance distributions in finite uniformly random networks: theory and applications. *IEEE Transactions on Vehicular Technology* 2010; **59**(2):940–949.
25. Haenggi M. Outage, local throughput, and capacity of random wireless networks. *IEEE Transactions on Wireless Communications* 2009; **8**:4350–4359.
26. Gong Z, Haenggi M. Mobility and fading: two sides of the same coin. *Proceedings of the 2010 Global Telecommunications Conference (GLOBECOM)*, Miami, FL, USA; 1–5.
27. Torrieri D, Valenti MC. The outage probability of a finite ad hoc network in Nakagami fading. *IEEE Transactions on Communications* 2012; **11**:3509–3518.

DOI: 10.1002/dac

28. Guo J, Durrani S, Zhou X. Outage probability in arbitrarily-shaped finite wireless networks. *IEEE Transactions on Communications* 2014; **62**(2):699–712.
29. Lee WY, Akyildiz IF. Optimal spectrum sensing framework for cognitive radio networks. *IEEE Transactions on Wireless Communications* 2008; **7**(10):38453857.
30. ETSI TS 125 101 V12.7.0 (2015-04). Available from: http://www.etsi.org/deliver/etsi_ts/125100_125199/125101/12.07.00_60/ts_125101v120700p.pdf (accessed November 26, 2015).
31. IEEE Standard 802.22-2011. Available from: http://www.ieee802.org/22/ (accessed November 26, 2015).
32. Le T, Mayaram K, Fiez T. Efficient far-field radio frequency energy harvesting for passively powered sensor networks. *IEEE Journal of Solid-State Circuits* 2008; **43**(5):1287–1302.
33. Tan Y K, Panda S K. Energy harvesting from hybrid indoor ambient light and thermal energy sources for enhanced performance of wireless sensor nodes. *IEEE Transactions on Industrial Electronics* 2011; **58**(9):4424–4435.
34. Sirkeci-Mergen B, Scaglione A, Mergen G. Asymptotic analysis of multistage cooperative broadcast in wireless networks. *IEEE Trans. Info. Theory* 2006; **52**(6):2531–2550.

DOI: 10.1002/dac